Supporting Information

Designing Reductive Hybrid Membrane to Capture Selectively Noble Metallic ions During Oil/Water Emulsion Separation with Further Function Enhancement

Lei Zhang,[a] Xianhu Zha,[b] Gui Zhang, [a] Jincui Gu,[a] Wei Zhang, [a] Youju Huang,*[a] Jiawei Zhang,[a] and Tao Chen*[a]

a Key Laboratory of Marine Materials and Related Technologies, Zhejiang Key Laboratory of Marine Materials and Protective Technologies, Ningbo Institute of Materials Technology and Engineering, Chinese Academy of Sciences, Ningbo 315201, China.

b Engineering Laboratory of Specialty Fibers and Nuclear Energy Materials, Ningbo Institute of Materials Engineering and Technology, Chinese Academy of Sciences, Ningbo, 315201, China.

* To whom correspondence should be addressed E-mail: tao.chen@nimte.ac.cn yjhuang@nimte.ac.cn;

Experimental Section

1. Preparation of the oil/water emulsion.

Oil-in-water emulsion: 5 g of emulsifier tween 80 (HLB = 15) was added into 500 mL of water, and then 15 mL of organic solvent (toluene, dichloromethane and chloroform, et al) was added. The mixture was stirred for 5 h and then left standing for 24 h until no de-emulsification was observed.

Oil-in-water emulsion containing metal ions: A certain amount of metal chloride or nitrate was dissolved into 500 mL of H_2O, respectively. 5 g of emulsifier tween 80 was added into the aqueous solution and stirred vigorously. Subsequently, 15 mL of toluene solvent was added. The mixture was stirred for 5 h and then left standing for 24 h until no de-emulsification was observed.

2. Extraction of noble metal ions during oil/water separation

20 mL of toluene/water emulsion containing different metal ions was added into the filtration setup. The vacuum degree was adjusted for tuning the flowing rate and retention time. Due to the underwater superoleophobic surface of composite membrane, the oil was obstructed while the water passed freely through the membrane. After separation, the composite membrane was emerged into ethanol to remove residual organic solvent and surfactant for further characterization. The filtrate was also collected to evaluate the oil/water separation performance.

3. Integration of hybrid membrane with electrode.

The diameter of prepared hybrid membrane is about 45 mm. Two copper foil electrode (width, 3 mm, thickness, about 0.065 mm) was adhesive onto the edge of composite membrane by the assistant of conductive resin. The contact area is keep constant about 5 mm ×3 mm (length × width). Besides, the membrane was fixed between two sealed spacer (polydimethylsiloxane, PDMS) with a central cavity (diameter about 2.8 cm). The structures of hybrid membrane integrated with copper electrode is shown as Scheme S1.

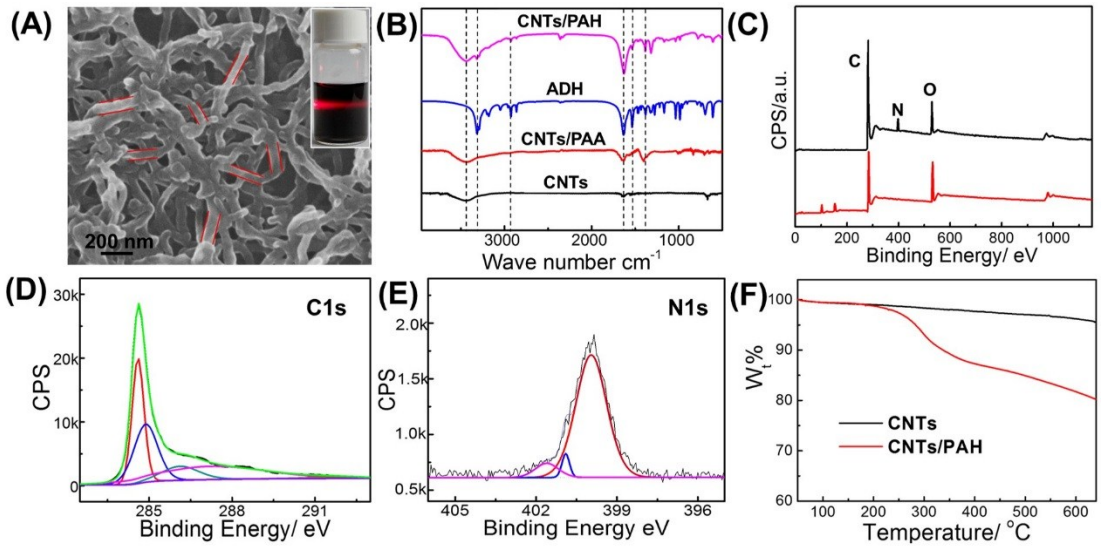

Fig. S1 The SEM image of CNTs/PAH. The inset shows the graph of CNTs/PAH dispersion in water. (B) The FT-IR spectra of CNTs/PAH. (C) X-ray photoelectron spectroscopy spectra of CNTs/PAH. (D) and (E) are C1s spectrum and N1s spectrum of CNTs/PAH. (F) The TGA curves of CNTs/PAH and pristine CNTs.

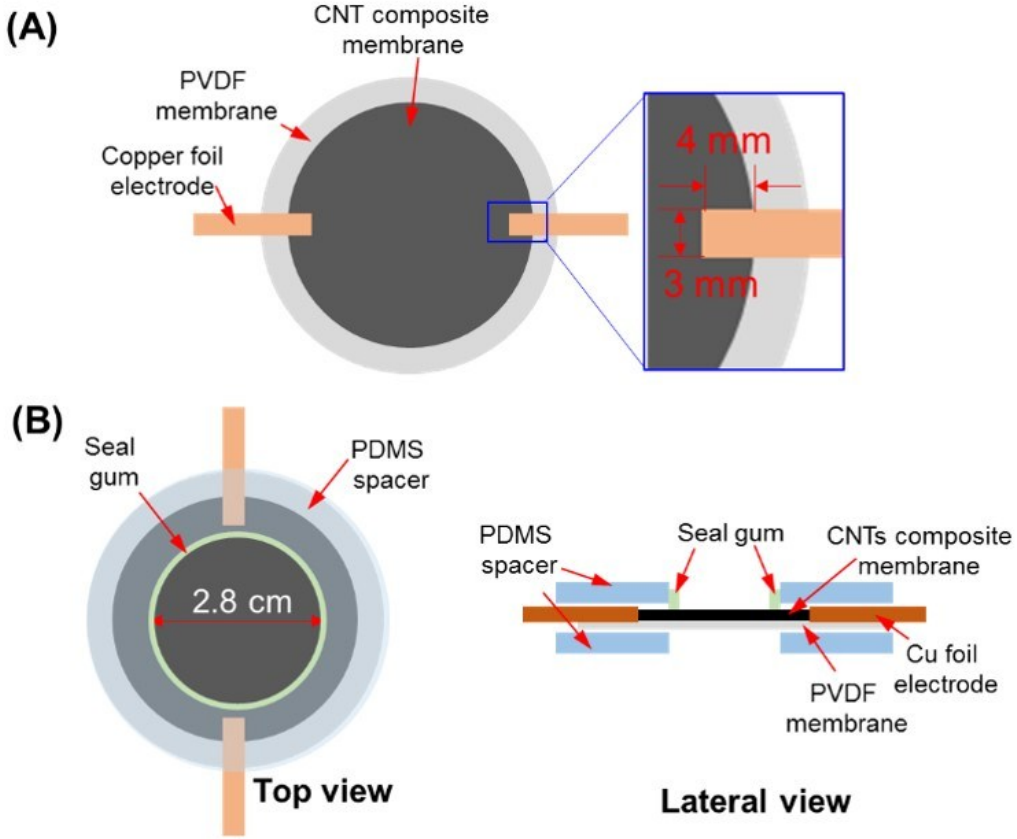

Scheme S1 The structures of hybrid membrane integrated with copper electrode (A) and its packaging using PDMS spacer (B).

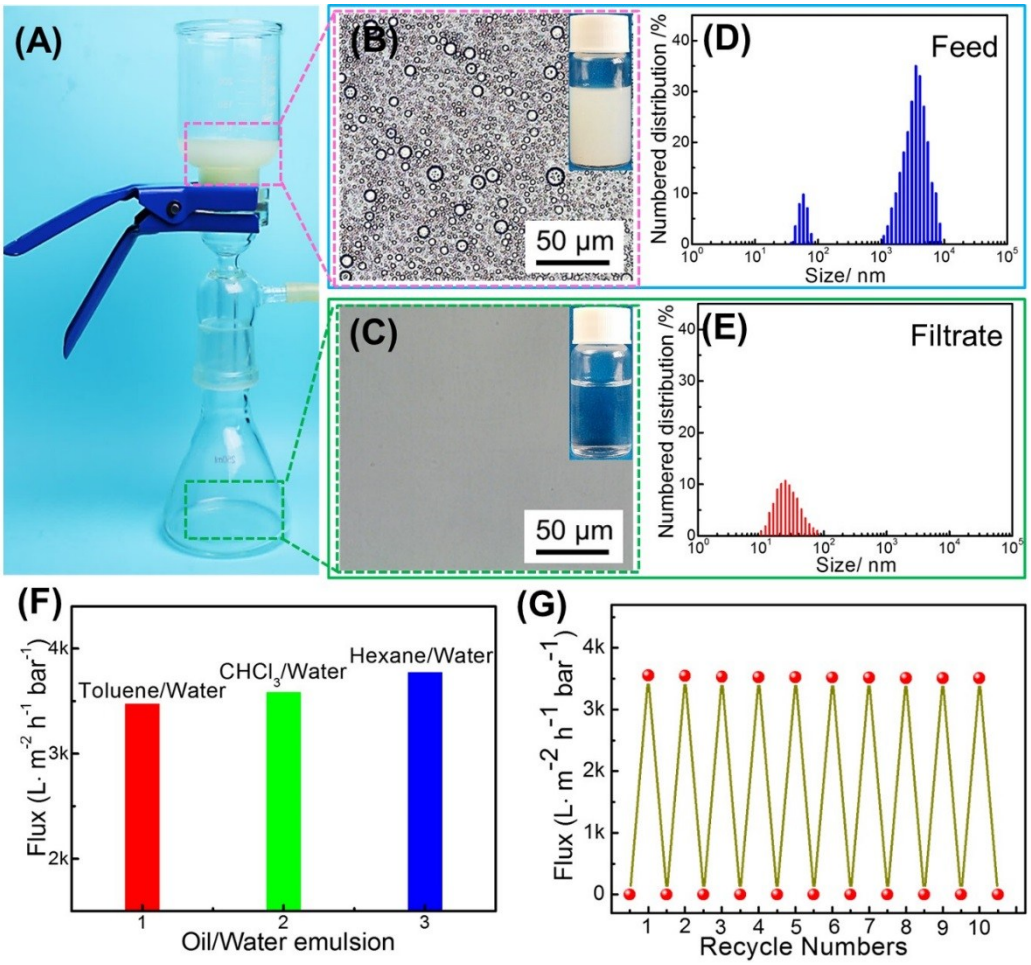

Fig. S2 (A) The setup of oil/water separation for CNTs/PAH hybrid membrane for separating toluene-in-water emulsions (3%, v/v). Optical microscopic pictures (B, C) and size distribution (D, E) of feed emulsion and filtrate solution. (F) Flux of toluene/water, chloroform/water and hexane/water emulsion passing through hybrid membrane. (G) Flux of separating toluene/water emulsion in different recycle numbers.

The content of toluene in filtrate solution was tested precisely by UV/vis absorption. A series of toluene-in-water mixtures with different content of toluene are prepared and stabilized with Tween 80 (0.4 w_t%). The plots of characteristic absorption of toluene at 250 nm against content were recorded and fitted linearly (Fig. S3). Their relationship can be described as y= 5.8□10-3 x + 0.002 (R= 0.985). the content toluene in filtrate solution (absorption intensity at 250 nm is about 4.3×10^{-3}) is about 0.39 mg/L.

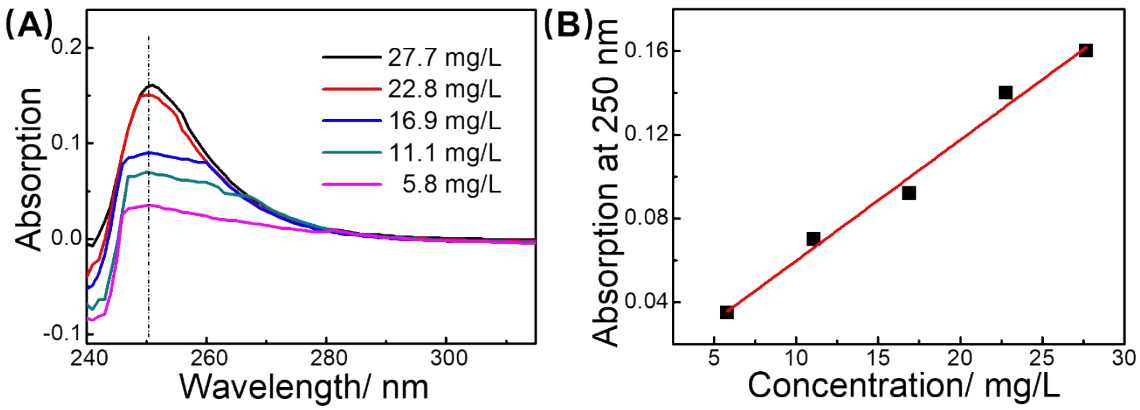

Fig. S3 (A) Absorption of toluene/water mixtures with different contents of toluene. (B) The plots of absorption at 250 nm against concentration of toluene and fitted linear curves.

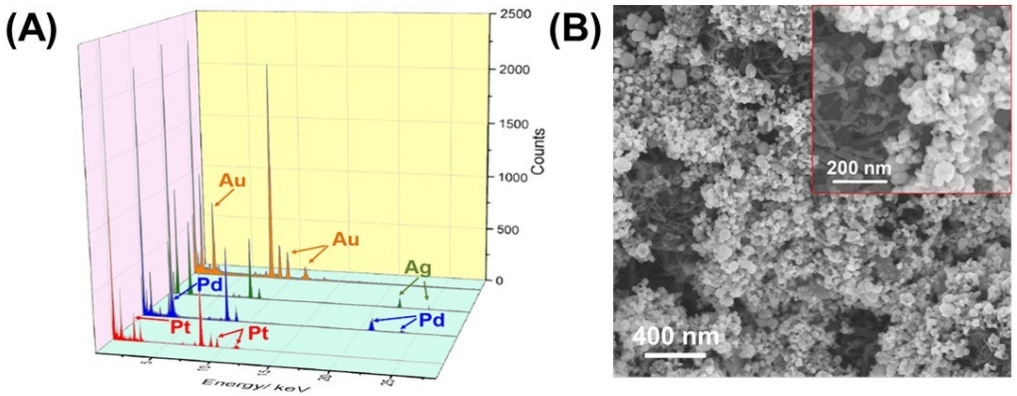

Fig. S4 (A) Energy dispersive spectroscopy of hybrid membrane extracting Au, Ag, Pd, and Pt ions respectively from toluene/water emulsion. (B) SEM images of hybrid membrane after treating mixed solution containing Au, Ag, Pd, and Pt ions (the contents of ions is kept at 5 mM).

$$2HAuCl_4+6C_{11}ON_2H_{22}+6H_2O=2Au+3N_2+6C_{11}O_2H_{20}+6NH_4Cl+2HCl$$
$$6AgNO_3+6C_{11}ON_2H_{22}+6H_2O=6Ag+3N_2+6C_{11}O_2H_{20}+6NH_4NO_3$$
$$PdCl_2+2C_{11}ON_2H_{22}+2H_2O=Pd+N_2+2C_{11}O_2H_{20}+2NH_4Cl$$
$$H_2PtCl_6+4C_{11}ON_2H_{22}+4H_2O=Pt+2N_2+4C_{11}O_2H_{20}+4NH_4Cl+2HCl$$
$$2FeCl_3+6C_{11}ON_2H_{22}+6H_2O=2Fe+3N_2+6C_{11}O_2H_{20}+6NH_4Cl$$
$$NiCl_2+2C_{11}ON_2H_{22}+2H_2O=Ni+N_2+2C_{11}O_2H_{20}+2NH_4Cl$$
$$CuCl_2+2C_{11}ON_2H_{22}+2H_2O=Cu+N_2+2C_{11}O_2H_{20}+2NH_4Cl$$
$$ZnCl_2+2C_{11}ON_2H_{22}+2H_2O=Zn+N_2+2C_{11}O_2H_{20}+2NH_4Cl$$

Fig. S5 The reduction reaction in the extraction of Au (III), Ag (I), Pd (II), and Pt (IV) ions.

Our first-principles calculations were implemented in the plane-wave VASP code.[1] The generalized gradient approximation (GGA) of Perdew–Burke–Ernzerhof (PBE) scheme was adopted for describing the exchange-correlation functional.[2] A plane-wave cutoff energy of 550 eV on basis of the projector augemented wave (PAW) pseudopotentials was employed.[3] During optimization, all the structures were relaxed until the forces on each atom were less than 1.0×10^{-2} eV/Å, and the convergence criterion for the total energy was set as 1.0×10^{-6} eV. Regarding to the k-point sampling, 1×1×4 Monkhorst-Pack[4] grids were adopted for our high-molecular polymers which periodicities are along the c-axis; only the Gamma point was adopted for small molecules. An enough vacuum space layer larger than 15 Å was employed in the nonperiodic directions. All the structures were visualized in the VESTA code.[5]

The metal complexes generally show line models or flat structures except for $HAuCl_4$ and H_2PtCl_6. For instance, the atoms in $AgNO_3$ are located on a plane with the distance between the silver and nitrogen atoms measured to be 2.681 Å. Line structures are generally determined in three-atoms molecules MCl_2 (M= Ni, Cu, Zn), but an obtuse angle of 100.5˚ is found in $PdCl_2$.

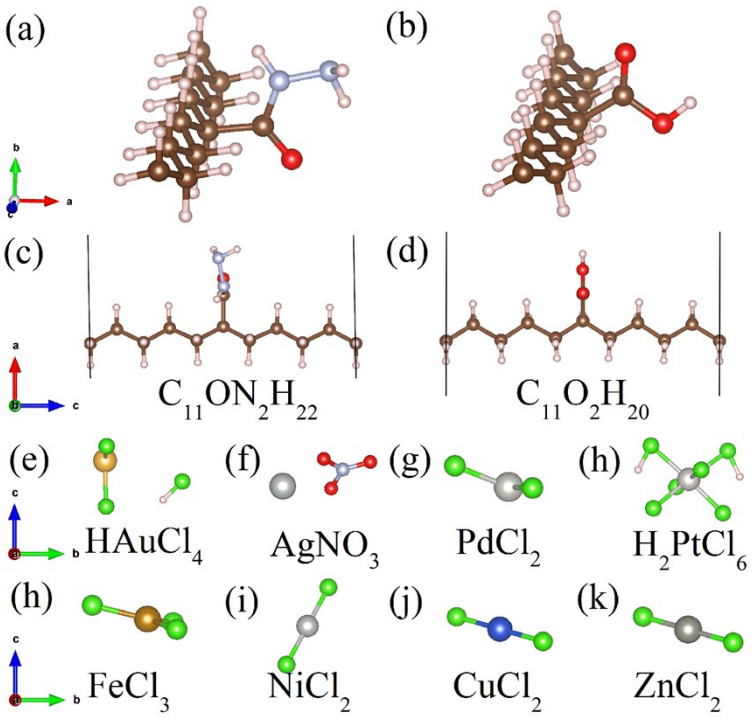

Fig. S6 The optimized structures for the reactants except for H_2O. (a) and (b) are the top-views for $C_{11}O_2H_{22}$ (simulated PAH analog) and $C_{11}O_2H_{20}$ (simulated reaction product of PAH); (c) and (d) are the corresponding side-views, the periodic direction is along the c-axis. (e)-(k) present the molecules $HAuCl_4$, $AgNO_3$, $PdCl_2$, H_2PtCl_6, $FeCl_3$, $NiCl_2$, $CuCl_2$, $ZnCl_2$, respectively.

Table 1 Gibbs energy for reduction reaction of each metal ions based on first-principles calculation.

Metal	Valence state	Gibbs energy (eV)
Au	Au(III)→ Au (0)	-13.39
Ag	Ag (I) → Ag (0)	-6.25
Pd	Pd(II) → Pd (0)	-1.41
Pt	Pt(IV) → Pt (0)	-1.44
Fe	Fe(III) → Fe (0)	6.44
Cu	Cu(II) → Cu (0)	0.33
Ni	Ni (II) → Ni (0)	1.36
Zn	Zn(II) → Zn (0)	0.57

Fig. S7 The recycling utilization of extracted Pd on CNTs composite membrane for catalytic decomposition of methylene blue during oil/water separation.

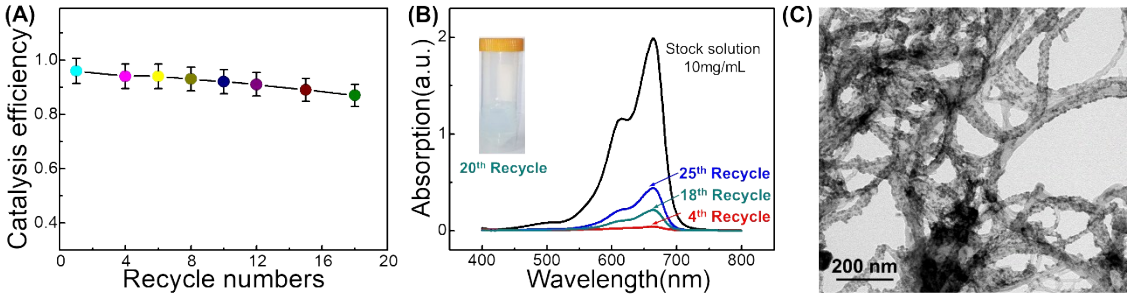

Fig. S8 (A) The catalytic efficiency variation after different times of recycling. (B) UV/vis absorption of filtration solution collected after 4 times, 18 times and 25 times of recycling. The inset shows the filtration solution after 20 times of recycling separation. (C) TEM image of CNTs/PAH membrane after 18th recycling.

References

[1] G. Kresse, J. Furthmüller, *Phys. Rev. B* **1996**, 54, 11169.

[2] J. P. Perdew, K. Burke, M. Ernzerhof, *Phys. Rev. Lett.* **1996**, 77, 3865.

[3] P. E. Blöchl, *Phys. Rev. B* **1994**, 50, 17953.

[4] H. J. Monkhorst, J. D. Pack, *Phys. Rev. B* **1976**, 13, 5188.

[5] K. Momma, F. Izumi, *J. Appl. Crystallogr.* **2011**, 44, 1272.